Proceedings of the ASME 2010 3rd Joint US-European Fluids Engineering Summer Meeting and 8th International Conference on Nanochannels, Microchannels, and Minichannels
FEDSM-ICNMM2010
August 1-5, 2010, Montreal, Canada

FEDSM-ICNMM2010-30323

FLUXMETRIC ANALYSIS OF CAR INCLINATION EFFECTS ON THE THERMAL MANAGEMENT OF UNDERHOOD TOP REGION

Mahmoud Khaled
Thermofluids, Complex Flows and Energy Research Group – Laboratoire de Thermocinétique, CNRS-UMR 6607, Ecole Polytechnique
University of Nantes
Nantes, France

Fabien Harambat
Aerodynamic and Aeroacoustic Research and Development Department – PSA Peugeot Citroen
Vélizy, France

David Hamadi
Thermofluids, Complex Flows and Energy Research Group – Laboratoire de Thermocinétique, CNRS-UMR 6607, Ecole Polytechnique
University of Nantes
Nantes, France

Anthony Yammine
Aerodynamic and Thermodynamic Research and Development Department – Kratzer Automation
Jouy en Josas, France

Hassan Peerhossaini
Thermofluids, Complex Flows and Energy Research Group – Laboratoire de Thermocinétique, CNRS-UMR 6607, Ecole Polytechnique
University of Nantes
Nantes, France

ABSTRACT

It is now well established that car inclination influences component temperatures in the car underhood compartment [1, 2]. This study presents an analysis of these effects by measurement of the heat flux that enters or leaves the underhood components. We report underhood thermal measurements carried out in wind-tunnel S4 of Saint-Cyr l'Ecole on a passenger vehicle. The underhood compartment is instrumented with 40 surface and air thermocouples and 20 fluxmeters of normal gradients. Three configurations of car positions are investigated: the flat, the up-hill and the down-hill inclinations. Measurements are carried out for three different car thermal functioning points.

Keywords: Underhood thermal management, Underhood top region, Car inclination, Convective and radiative heat flux, Temperature, Wind tunnel, Automotive.

INTRODUCTION

A vehicle adopts different inclinations according to the different loadings (masses) applied to it (Figure 1a): flat (horizontal), uphill and downhill inclinations. Also, an empty car is not necessarily in a flat position (statistics for the initial inclinations of some cars are shown in Figure 1b).

These inclinations impose incidence angles on the airflow entering the underhood region through the air inlet openings. Then, since the airflow into the underhood strongly affects the cooling of the underhood components, car inclination can affect the underhood aerothermal situation, especially in the center and bottom regions.

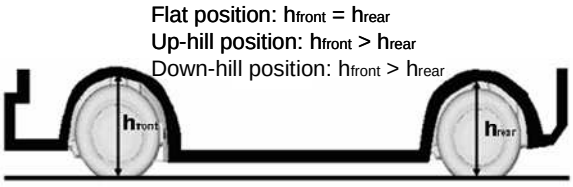

(a)

	Initial inclination	h rear (cm)	h front (cm)
BMW 5 series	Down-hill	68.6	68
Mercedes CLC220	Up-hill	66	67.5
Citroën C4	Down-hill	70	69.5
Peugeot 307 SW	Up-hill	68.6	69.4
Golf	Down-hill	68.3	66
Ford FOCUS	Up-hill	64.5	65.4
Toyota PRJUS	Up-hill	65	66

(b)

Figure 1: (a) Car inclinations; (b) initial inclinations of different car series.

On the other hand, in previous underhood aerothermal studies, car inclination was not controlled in the experimental investigations, nor was it considered in the numerical simulations. It has been shown ([1]) that uphill and downhill inclinations increase the underhood temperatures in both the constant-speed driving and thermal soak phases. In addition, most work has focused especially on the middle and bottom regions of the underhood ([2]). However, we have measured nontrivial temperatures increases at some positions of the underhood top region, even though in this region the air flow is very strong. Several questions thus arise from these observations: do these effects exist for the entire underhood top region? If so, for what reasons? Do these temperature effects vary with car speed?

To answer these questions, aerothermal investigations were performed on a passenger car in wind tunnel S4 of Saint-Cyr l'Ecole. Experiments were carried out for three different thermal functioning points (three different values for wind tunnel air velocity and engine power) and the underhood was instrumented by 40 surface and air thermocouples and 20 fluxmeters of normal gradients. During experiments, the engine entrains power control-absorption rollers.

This investigation had two steps:
- a first step in which the effects of car inclination on the component temperatures in the underhood top region are investigated; variations in the overall heat flux densities at component surfaces are also studied,
- a second step in which variations of the overall heat flux densities are analyzed in terms of radiative and convective densities separately. For this purpose a special flux measurement technique was used that allows separate simultaneous measurement of the convective and radiative heat flux on one point in the underhood compartment [3-5].

The rest of this paper is organized as follows. The next section lays out the theoretical basis of the specific method of separated convective-and-radiative heat flux measurement and describes the experimental method and the underhood instrumentation d. The following section presents the results and physical analysis of the aerothermal effects of inclination provided by the separate measurements of the convective and the radiative heat flux densities.

NOMENCLATURE

EAS	electronic assisted steering
CAC	charge air cooler
f	form factor
h	heat transfer coefficient, $W.m^{-2}.K^{-1}$
n	engine regime, rpm
P	wheel power, KW
R	gear ratio
T	temperature, $°C$
TFP-1	thermal functioning point 1
TFP-2	thermal functioning point 2
TFP-3	thermal functioning point 3
V	car speed, $Km.h^{-1}$
WOP	water outlet plenum

Greek symbols

φ	flux density, $W.m^{-2}$
ε	emissivity
σ	Stefan-Boltzmann constant, $W.m^{-2}.K^{-4}$

Subscripts and superscripts

a	air
c	convective
ov	overall
r	radiative
S	surface
W	wheel
0	characteristic
1	fluxmeter 1 or black fluxmeter
2	fluxmeter 2 or aluminum fluxmeter

THEORETICAL BASIS

The method for measuring the convective and radiative heat fluxes consists in attaching to a surface of emissivity ε_S two fluxmeters of different emissivities ε_1 and ε_2 (in practice, one solution is to paint a fluxmeter with black paint and the other with aluminum paint). Details on the operating principle

of the method as well as its precision and sensitivity can be found in [3]; here a short account of these details is given below.

In most thermal applications, such as in underhood applications, convective and radiative heat transfers occur simultaneously. In these cases, measured heat fluxes are the overall heat fluxes corresponding to the sum of the convective and radiative heat fluxes:

$$\varphi = \varphi_c + \varphi_r \quad (1)$$

The convective and the radiative heat fluxes are generally expressed as follows:

$$\varphi_c = h_c\left(T_S - T_a\right) \quad (2)$$
$$\varphi_r = \varepsilon\sigma\left(T_S^4 - T_r^4\right) \quad (3)$$

Then, the overall heat flux is given by:

$$\varphi = h_c\left(T_S - T_a\right) + \varepsilon\sigma\left(T_S^4 - T_r^4\right) \quad (4)$$

When two fluxmeters of different emissivities ε_1 and ε_2 are used on a surface of emissivity ε_S, they measure different overall heat fluxes as follows:

$$\text{Fluxmeter 1: } \varphi_1 = h_{c1}(T_{s1} - T_a) + \varepsilon_1\sigma\left(T_{s1}^4 - T_r^4\right) \quad (5)$$
$$\text{Fluxmeter 2: } \varphi_2 = h_{c2}(T_{s2} - T_a) + \varepsilon_2\sigma\left(T_{s2}^4 - T_r^4\right) \quad (6)$$

The surface temperatures and the convective heat transfer coefficient measured by the two fluxmeters are considered to be approximately the same:

$$T_{S1} = T_{S2} = T_S \quad (7)$$

$$h_{c1} = h_{c2} = h_c \quad (8)$$

Then, from the two experimental points $(\varepsilon_1;\varphi_1)$ and $(\varepsilon_2;\varphi_2)$ in the $(\varepsilon;\varphi)$ plane, one can deduce the linear variation of the overall heat flux φ_{ov} with the surface emissivity ε_S $\varphi_{ov} = f(\varepsilon_S)$:

$$\varphi = f(\varepsilon) = \left[\frac{\varphi_2 - \varphi_1}{\varepsilon_2 - \varepsilon_1}\right]\varepsilon + \left[\varphi_1 - (\varphi_2 - \varphi_1)\frac{\varepsilon_1}{\varepsilon_2 - \varepsilon_1}\right] \quad (9)$$

After that, one can determine the different parameters as follows:

$$\varphi_c = f(0) = \varphi_1 - (\varphi_2 - \varphi_1)\frac{\varepsilon_1}{\varepsilon_2 - \varepsilon_1} \quad (10)$$

$$\varphi_g = f(\varepsilon_s) = \left[\frac{\varphi_2 - \varphi_1}{\varepsilon_2 - \varepsilon_1}\right]\varepsilon_s + \left[\varphi_1 - (\varphi_2 - \varphi_1)\frac{\varepsilon_1}{\varepsilon_2 - \varepsilon_1}\right] \quad (11)$$

$$\varphi_r = f(\varepsilon_s) - f(0) = \left[\frac{\varphi_2 - \varphi_1}{\varepsilon_2 - \varepsilon_1}\right]\varepsilon_s \quad (12)$$

$$T_r = \sqrt[4]{T_s^4 - \frac{f(\varepsilon_s) - f(0)}{\varepsilon_s\sigma}} = \sqrt[4]{T_s^4 - \frac{1}{\sigma}\left[\frac{\varphi_2 - \varphi_1}{\varepsilon_2 - \varepsilon_1}\right]} \quad (13)$$

EXPERIMENTS

The experimental procedure and test configurations are presented in detail in [6-7]; below a short account of this procedure and the underhood instrumentation is given.

Experimental procedure

Aerothermal investigations were carried out on a vehicle in the wind-tunnel of Saint-Cyr l'Ecole. The car engine is entrained to front-wheel rollers that permit adjustment and control of the wheel power and rotational speed. Investigations were carried out for the three thermal functioning points described in table 1.

	V_W km.h^{-1}	V_{wind} km.h^{-1}	P kW	R -	n rpm
TFP-1	90	90	69	5	2600
TFP-2	110	55	89	4	3800
TFP-3	130	130	98	5	3780

Table 1: Parameters defining the three thermal functioning points.

Three car inclination configurations are investigated: the flat, uphill, and downhill inclinations. For each investigation (fixed car inclination and thermal functioning point), data recording (heat flux and temperatures) covers three successive phases: the constant-speed driving, slow-down, and thermal soak phases. The constant-speed driving phase simulates the actual driving of a vehicle and can be TFP-1, TFP-2, or TFP-3. The slowdown phase is simulated in the wind tunnel by passing to the neutral point after the constant-speed driving phase and by stopping the wind-tunnel airflow. Thermal soak corresponds to the stopping of the vehicle after a high thermal charge.

Instrumentation

The car underhood is instrumented with 40 surface and air thermocouples and 20 fluxmeters of normal gradients. The instrumented regions are essentially: side of the cold box (zone including the battery and the calculator), upstream and above the cold box, the air filter; the cylinder head cover, the charge air cooler (CAC) inlet duct, the engine right side, and the CAC outlet duct. The heat flux sensors for separate convective and radiative measurements are instrumented by pairs. Figure 2 show examples of instrumentation (with surface thermocouples, air thermocouples, and fluxmeters) at the cylinder head cover, above the cold box, and the CAC inlet and outlet ducts.

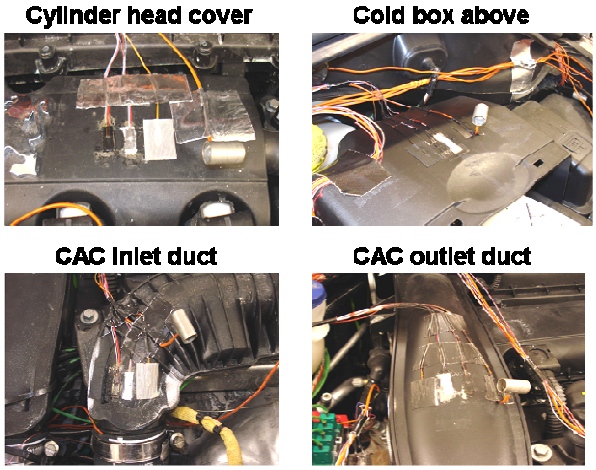

Figure 2: Underhood instrumentation with fluxmeters, surface thermocouples and air thermocouples.

RESULTS AND ANALYSIS

From temperature and heat flux (global, convective, and radiative) measurements, it was observed that:

1- In the constant-speed driving phase, car inclination affects component temperatures (increases) in the underhood top region, but less significantly than in the underhood middle and bottom regions. On the other hand, these effects in the thermal soak phase are of the same order in all underhood regions (top, middle and bottom).

2- It is difficult to establish a coupling between temperature and overall heat flux evolution in looking at the thermal effects of inclination.

3- Analysis of the car inclination effects based on the separate measurements of convective and radiative heat fluxes is more straightforward and permits elucidation of the effects of some parameters that is impossible from overall heat flux measurements (for example, the combined effect of car inclination and exterior air flow speed).

The above findings are detailed in the following subsections.

Effects of car inclination on temperatures of the underhood top region

By comparing the different inclinations and temperature variations at the different components in the underhood top region, it was found that uphill and downhill inclinations increase the underhood temperature not only in the middle and bottom regions [6-7] but also in the top region. As an example, Figure 3 shows temperature variations for the three inclinations investigated on a component (the triangle) in the middle and bottom regions of the underhood, and another component in the top region (the air filter).

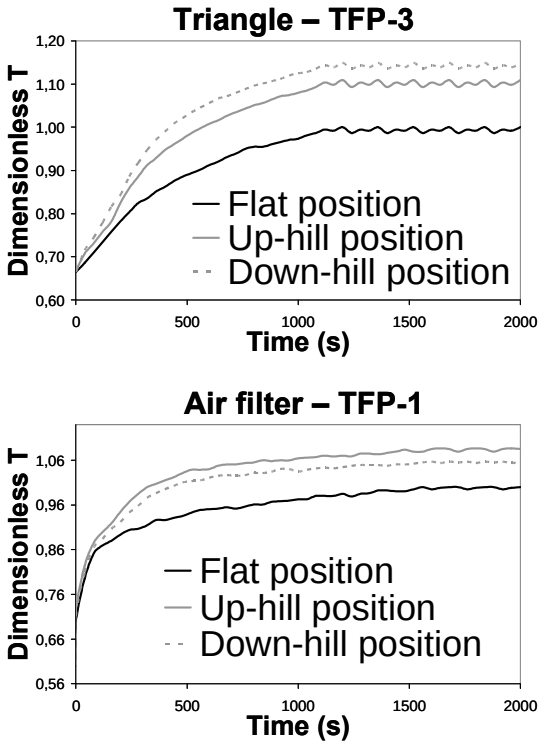

Figure 3: Effects of inclination on temperature variations.

It is observed that the uphill and downhill inclinations increase both the temperature of the triangle and that of the air filter but less significantly in the air filter (situated in the top region). For example, for the uphill inclination with respect to a relative temperature of 1.06 T_{flat} measured at the air filter, a temperature of 1.15 T_{flat} was measured at the triangle at the end of the constant-speed driving phase.

By calculating the relative temperature difference due to the car inclination (with respect to the effect identified by the quantitative method [1, 2] in the constant-speed driving phase and the thermal soak phase, it is observed that car inclination increases the temperature of the underhood top region in both the constant-speed driving and thermal soak phases. However, comparing the relative temperature differences caused by car

inclination shows that the effects of car inclination on temperatures in the underhood top region in the constant-speed driving phase are less significant than in the middle and bottom regions.

Figure 4 shows the relative temperature differences due to the uphill and downhill inclinations in the constant-speed driving phase for respectively the underhood top region components (Figure 4a) with $\left|h_{front} - h_{rear}\right| = 1.5\,cm$ and the middle and bottom underhood region components with $\left|h_{front} - h_{rear}\right| = 1\,cm$.

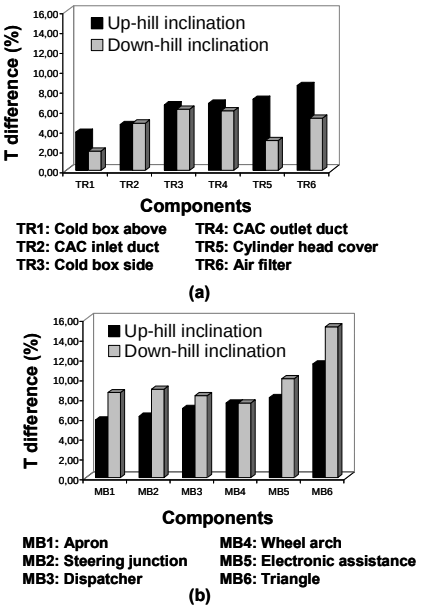

Figure 4: Relative temperature differences due to uphill and downhill inclinations in constant-speed driving phase for components in: (a) underhood top region ($h_{front} - h_{rear} = \pm 1.5$ cm) and (b) underhood middle and bottom regions ($h_{front} - h_{rear} = \pm 1.0$ cm).

It is observed that the car inclinations (uphill or downhill) increase the temperatures at several positions throughout the underhood top region with respect to the flat position in the constant-speed driving. The relative temperature differences in the top region (Figure 4a) due to the uphill and downhill inclinations are smaller than those in the middle and the bottom regions (Figure 4b). For example, the relative temperature differences due to the uphill inclination in the underhood top region vary from 3.9% at the cold-box upper face to 8.6% at the air filter. In the middle and the bottom regions, relative temperature differences range from 5.8% at the apron to 11.5% at the triangle. For the downhill inclination in the top region, temperature differences range from 1.9% above the cold box to 6.15% at the cold-box side. In the middle and bottom regions, these differences range from 8.6% at the oil pipe to 15.2% at the triangle.

Figure 5 shows relative temperature differences due to uphill and downhill inclinations, this time in the thermal soak phase for the underhood top region components (Figure 5a) with $\left|h_{front} - h_{rear}\right| = 1.5\,cm$ and the middle and bottom underhood regions components with $\left|h_{front} - h_{rear}\right| = 1\,cm$ (Figure 5b).

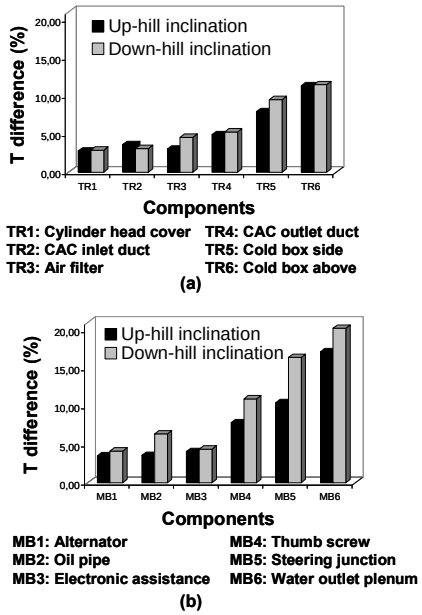

Figure 5: Relative temperature differences due to uphill and downhill inclinations in the thermal soak phase for components in: (a) underhood top region region ($h_{front} - h_{rear} = \pm 1.5$ cm) and (b) underhood middle and bottom regions ($h_{front} - h_{rear} = \pm 1.0$ cm).

It is seen that the car inclinations increase the temperature in the underhood top region in thermal soak, too. These effects are also smaller in the underhood top region than in the middle and bottom regions. As an example, one observes that in the top region, the relative temperature differences due to the downhill inclination range from 2.9% at the cylinder head cover to 11.5% above the cold box. In the middle and bottom regions, these differences range from 4.2% at the alternator to 20.3% at the water outlet plenum (WOP).

Relation between overall heat flux and temperatures evolution

In order to analyze the temperature increases at the underhood top region induced by car inclination, we start by looking at the evolution of the overall heat flux densities and their relation with component temperatures. Figure 6 shows respectively the temperatures (Figure 6a) and the overall heat flux densities

(Figure 6b) at the different positions in the constant-speed driving phase. The values are nondimensionalized by the corresponding values in the flat car position.

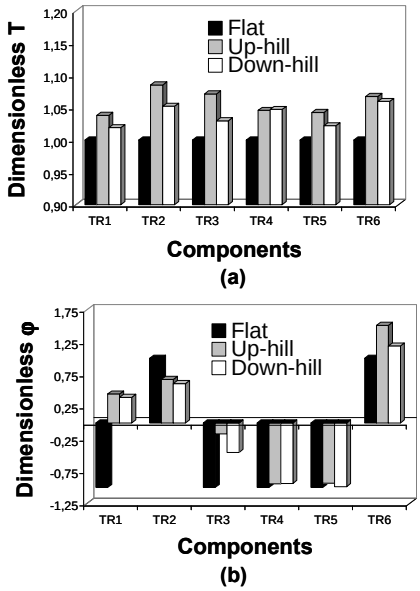

TR1: Cold box
TR2: Air filter
TR3: Cylinder head cover
TR4: CAC inlet duct
TR5: Engine right side
TR6: CAC outlet duct

Figure 6: (a) Dimensionless temperatures and (b) dimensionless overall heat fluxes at the different positions for the different car inclinations.

It is noted that uphill and downhill inclinations (Figure 6b) increase the absorbed (positive) overall heat flux and decrease the absolute value of the evacuated (negative) overall heat flux. In addition, these modifications are more significant for the uphill than for the downhill inclination This explains why temperatures for the uphill and downhill inclinations are higher than in the flat position, and also why the uphill temperatures are higher than the downhill temperatures. For example, at the CAC outlet duct, with respect to an overall heat flux φ_0 for the flat inclination, $1.51\varphi_0$ is measured for the uphill inclination and $1.19\varphi_0$ for the downhill inclination. With these increased absorbed overall heat fluxes for the uphill and downhill inclinations, temperatures are $1.07T_0$ for the uphill inclination and $1.06T_0$ for the downhill inclination with respect to a temperature T_0 for the flat inclination.

Analysis based on separate convective and radiative heat flux measurements

The effects of car inclination on the underhood top region temperatures described above are the consequence of modifications in convective heat transfer that change the radiative heat transfer, resulting in increases in the absorbed overall heat flux and decreases in the evacuated overall heat flux. Figure 7 shows an example of convective and radiative heat flux variations at the cold box side. Here all heat fluxes have been nondimensionalized by the overall heat flux measured at t = 0 for the flat position.

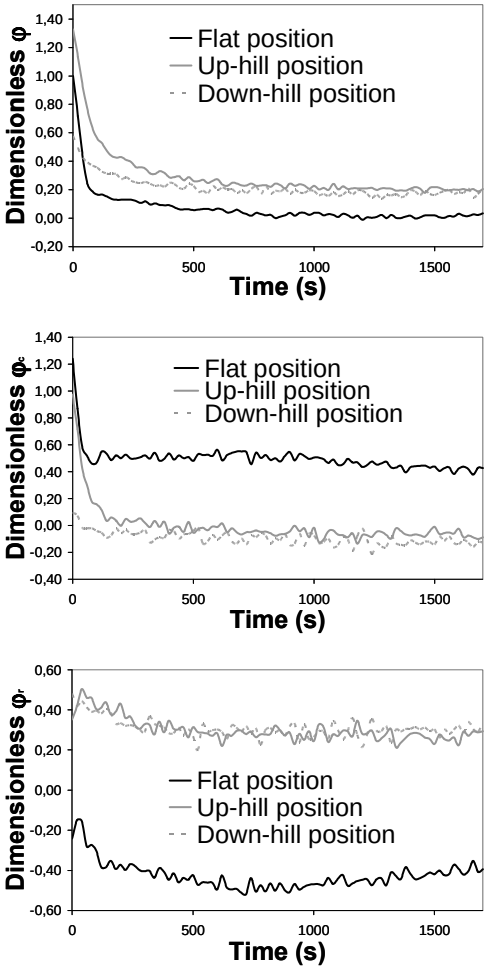

Figure 7: Heat flux variation at the cold box side for different car inclinations in constant-speed driving phase.

It is noted that, with respect to a quasi-stabilized convective heat flux of $0.47\varphi_0$ for the flat position, a convective heat flux of $-0.06\varphi_0$ is measured for the uphill inclination and $-0.12\varphi_0$ for the downhill inclination. On the other hand, with respect to a quasi-stabilized radiative heat flux of $-0.45\varphi_0$ for the flat position, radiative heat fluxes of $0.27\varphi_0$ are measured for the uphill inclination and $0.29\varphi_0$ for the downhill inclination. The increase, indeed sign change of the radiative

heat flux due to the uphill and downhill inclinations dominates the decrease in the convective heat flux, resulting in an increase in overall heat flux (and therefore temperature). In addition, the downhill inclination favors convective heat transfer more than the uphill inclination. Then, with the same magnitude of radiative heat flux density augmentation between the downhill and uphill inclination, the uphill inclination increases the overall heat flux (temperature) more than the downhill inclination. This is why with respect to a quasi-stabilized overall heat flux of $0.02\varphi_0$ in the flat position, an overall heat flux of $0.21\varphi_0$ was measured for the uphill inclination and $0.18\varphi_0$ for the downhill inclination.

These thermal behaviors are also observed for all the positions investigated: in the constant-speed driving phase, the uphill and downhill inclinations promote convective heat transfer and reduce radiative heat transfer. The radiative heat transfer reduction usually dominates the improvement in convective heat transfer, resulting in augmentation of the absorbed (positive) overall heat flux or a decrease in absolute value of the evacuated overall heat flux.

Figure 8 shows the convective (Figure 8a) and the radiative (Figure 8b) heat flux densities at different positions and for different car inclinations in the constant-speed driving phase. It is noticed that uphill and downhill inclinations increase the absolute values of the evacuated (negative) convective heat flux. For the absorbed (positive) convective heat flux, they may change the sign, increase or decrease it. In fact, adopting a positive sign convention for an absorbed convective heat flux lets it be written as follows:

$$\varphi_c = h_c.(T_a - T_S) \quad (14)$$

Uphill and downhill inclinations increase the convective heat transfer coefficient at different positions in the underhood top region. These convective coefficient increases compensate for the augmentation of the air temperature T_a with respect to the surface temperature T_S, giving rise to a slight reduction in the temperature difference $(T_a - T_S)$. Then, the increase in the convective heat transfer coefficient dominates the slight reduction of the temperature difference, resulting in an augmentation in absolute value of the evacuated (negative) convective heat flux. In addition, the downhill inclination increases the convective coefficient more than the uphill inclination. Therefore, with temperature difference increases of the two inclinations very close, the downhill inclination tends to increase the absolute value of the evacuated convective heat flux more than the uphill.

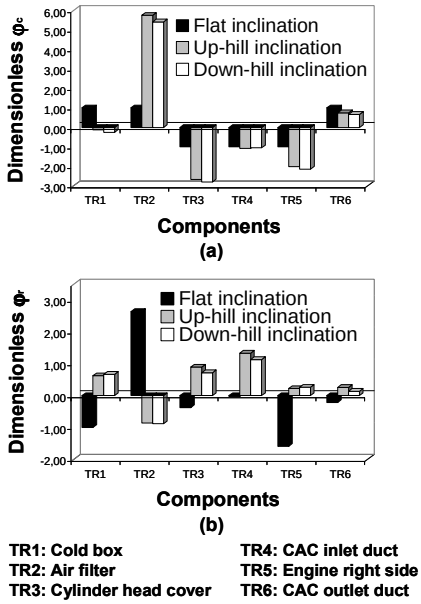

Figure 8: Evolutions at the different investigated positions in constant-speed driving for the different inclinations of the: (a) convective heat flux (b) radiative heat flux.

The same analysis is valid for the absorbed convective heat flux. A remarkable case is that of the cold box, for which the uphill and downhill inclinations change the sign of the exchanged convective heat flux. In fact, at this position, the uphill and downhill inclinations increase the convective coefficients in such a way that the augmentation of the fluid temperature becomes very limited with respect to that of the surface, resulting in sign changes in the temperature differences. Therefore, with slight negative temperature differences, the uphill and downhill inclinations change the sign of the convective heat flux and decrease its absolute value. On the other hand, an exception is observed at the CAC outlet duct, where the convective heat transfer coefficient decreases for the uphill and downhill inclinations. These convective coefficient decreases dominate the increase in temperature difference, resulting in a decrease in the convective heat flux densities.

The radiative heat flux variations with the different inclinations cannot be predicted as the convective heat flux variations can. These variations depend essentially on the component position and the thermal situation of its environment. In fact, the radiative heat flux exchanged at the surface of a component is given by the following expression:

$$\varphi_r = \sigma.\varepsilon.(T_r^4 - T_S^4) \quad (15)$$

where T_r is the mean radiative temperature of the component environment, which takes into account the different temperatures surrounding the component and the different form

factors of this component with respect to the different surrounding components:

$$T_r = \sqrt[4]{f_i . T_i^4} \quad (16)$$

where $f_i (i = 1 \rightarrow n)$ are the form factors of the element to the n surrounding components of temperatures T_i. Equation (15) shows clearly that the variation in radiative heat flux with the different car inclinations cannot be predicted and depends essentially on the augmentation rate of the two temperatures T_S and T_r. Figure 8b shows that the uphill and downhill inclinations change the sign of the evacuated radiative heat flux exchanged in the flat inclination. In fact, as shown in previous sections, the underhood top region is the zone whose temperature is least affected by car inclinations Therefore, the uphill and downhill inclinations increase the temperature T_r of a component in the top region more than its temperature T_S, since the temperature T_r represents some components in the top region and some in the middle region (even the bottom) in which the effects of car inclination on temperature are more significant.

Finally, with respect to the flat car position, the uphill and downhill inclinations improve convective heat transfer and influence the radiative heat transfer in the underhood top region. The impact on radiative heat flux always dominates the enhancement of the convective heat flux densities. This results in an augmentation of the overall heat flux exchanged at different surfaces, which causes a large part of the temperature increases observed in the underhood top region. In addition, the improvement in the convective heat transfer with the downhill inclination is more significant than with the uphill inclination. The reduction of the radiative heat transfer is of the same order in the uphill and downhill inclinations. This causes overall heat flux for the uphill inclination to be below that of the downhill inclinations. This is why more significant temperature increases have been observed for the uphill inclination, contrary to the trends of component temperatures in the middle and bottom regions.

CONCLUSIONS

Car inclination increases underhood temperatures in both the constant-speed driving and the thermal soak phases. These effects are of the same order in the two phases and are of different orders in the different underhood regions in the constant-speed driving phase. The underhood top region is the region least influenced by the car inclinations.

For most of the positions investigated in the underhood top region, the car inclinations improve convective heat transfer and reduce radiative heat transfer. The radiative heat transfer reduction dominates the convective heat transfer improvement, resulting in augmentation of the overall heat flux as well as temperature.

Finally, convective and radiative heat transfer modes always occur simultaneously in most thermal applications, particularly in automotive applications. It has been shown that separate measurement of the contribution of each mode to the overall heat flux densities is a key element in the physical understanding of the thermal behavior of the underhood compartment.

REFERENCES

[1] M. Khaled, F. Harambat and H. Peerhossaini, Effects of car inclination on air flow and aerothermal behavior in the underhood compartment, Proceedings of the ASME Fluids Engineering Conference, July 30-August 2, San Diego, CA, USA (2008), FEDSM2008-55093.

[2] M. Khaled, F. Harambat and H. Peerhossaini, A quantitative method for the assessment of car inclination effects on thermal management of the underhood compartment, J. Thermal Science and Engineering Applications, ASME, 1 (2009) 014501: 1-5.

[3] M. Khaled, B. Garnier, F. Harambat and H. Peerhossaini, A new method for simultaneous measurement of convective and radiative heat flux in car underhood applications, Meas. Sci. Technol. 21 (2010), 025903.

[4] M. Khaled, F. Harambat and H. Peerhossaini, Underhood thermal management: Temperature and flux measurements and physical analysis, Applied Thermal Engineering, 30 (2010), 590-598.

[5] RC01 Radiation/Convection (RADCON) Heat Flux Sensor, HUKSEFLUX™ THERMAL SENSORS Brochure.

[6] M. Khaled, F. Harambat and H. Peerhossaini, Temperature and heat flux behavior of complex flows in car underhood compartment, Heat Transfer Engineering (2010), in press.

[7] M. Khaled, F. Harambat, A. Yammine, and H. Peerhossaini, Optimization and active control of the underhood cooling system – a numerical analysis, Proceedings of the ASME 2010 3rd Joint US-European Fluids Engineering Summer Meeting and the 8th International Conference on Nanochannels, Microchannels and Milichannels, August 1-5, Montreal, Canada (2010).